ARTICLE NO. 80-4007

Radiation from Particles Injected into Hypersonic Flowfields

Nelson H. Kemp* and George E. Caledonia†
Physical Sciences Inc., Woburn, Mass.

This paper describes a model for the calculation of radiation from small particles injected into the wake of a hypersonic vehicle. The analysis extends the calculation of such radiation from the free molecular regime, previously modeled, to the full range of flow regimes appropriate to altitudes from 150 to 10 km. The model is based on the particle dynamics and heating from free molecule flow to continuum flow, and the thermal and radiative properties of the particle material. Calculations have been performed for particles of carbon, SiC and WC, from 150 to 10 km. Results show that under certain conditions the particle radiation may be enhanced by the higher density gas at lower altitudes.

Nomenclature

C = specific heat of solid
C_D = drag coefficient
C_{DV} = vehicle drag coefficient
C_{DF} = friction drag coefficient
D = drag
E_p' = time integrated particle in-band radiation normalized by initial particle mass
H = altitude
h = enthalpy per unit mass
M = Mach number
M_p = particle mass
$\mathcal{Q}$ = heat content of particle
$\dot{\mathcal{Q}}$ = collisional particle heating rate per unit surface area
r = radial coordinate from axis of vehicle
R_p = particle radius
R_w = density-weighted radial coordinate
T = temperature
U_x = axial gas velocity component relative to vehicle
U_r = radial gas velocity component relative to vehicle
$\overline{U}$ = average wake velocity to linearized wake integrals
v = mean thermal speed
V_{rel} = velocity of particle relative to flowing gas
x = axial coordinate from base of vehicle
α_v = sticking coefficient (vaporization)
ΔH_v = heat of vaporization per unit mass
ϵ = total emissivity
θ = angle of injection of particle relative to vehicle axis
ρ = mass density
σ = Stefan-Boltzmann constant

Subscripts

C = continuum flow
e = wake edge
FM = free molecular flow
p = particle
v = vapor
∞ = freestream

Received March 27, 1979; revision received July 24, 1979.

Index categories: Radiation and Radiative Heat Transfer; Rarefied Flows; Jets, Wakes, and Viscid-Inviscid Flow Interactions.

*Principal Scientist. Associate Fellow AIAA.
†Principal Scientist.

I. Introduction

IT has long been recognized that a re-entry vehicle undergoes aerodynamic heating as it traverses the atmosphere. It is clear that small particles injected from a re-entry vehicle into the flowfield will also experience such aerodynamic heating, albeit on a different scale. This mechanism could be exploited to provide for the generation of enhanced optical signatures from such particles which could be injected cold, as an aerosol, or heated, through use of a pyrotechnic generator. In the past, predictions of the anticipated radiation levels from such injected particles have been made in the exo-atmospheric limit, i.e., under conditions where interactions between the injected particles and ambient gases may be neglected. It has been realized, however, that this particle/gas interaction can result in significant changes in the particle signature. Indeed, studies of this effect,[1,2] in the limit of free molecular flow, demonstrated that this endo-atmospheric interaction could provide for a significant degree of radiation enhancement above the exo-atmospheric levels.

The purpose of the present paper is to examine the radiative/heating behavior of small particles upon their injection into hypersonic flowfields. The study has been performed over the full range of flow regimes appropriate to the altitude region of 150-10 km, and special care has been taken to provide realistic descriptions of the appropriate re-entry flowfields. Infrared radiative signature predictions have been performed for a wide variety of conditions in order to determine the effect of various particle and injection parameters (such as size, temperature, injection angle, etc.) on radiative performance.

The basic phenomenology and defining equations of the gas/particle interaction are presented in Sec. II. A description of analytic models for describing two-dimensionally varying laminar and turbulent wakes is also given in this section. The analysis of Sec. II has been utilized to develop a computer model, which provides predictions of particle radiation signatures for various re-entry scenarios. Such predictions are described in Sec. III for a wide variety of particle injection and flow conditions. The conclusions of the study may be found in Sec. IV.

II. Modeling of the Particle/Gas Interaction

Phenomenology

We are concerned with the injection, from the base of a re-entry vehicle, of small, micron-sized particles. The particles, initially either cold or heated, are injected at a velocity small relative to that of the vehicle. They then find themselves in a

flowfield traveling at hypersonic speed relative to them, since most of the gas around a re-entry vehicle is flowing at high speed. The ensuing gas/particle interaction is perhaps best envisaged in the free molecular flow limit where the concepts of elementary kinetic theory may be employed. In this limit, when gas molecules collide with the particles, a certain fraction of the collisions will be inelastic, or accommodating, in that the molecular velocity and temperature after the collision will be equal to that of the particle. In such collisions the change of energy of the molecule will, of course, be reflected by an equal and opposite change in the energy of the particle. The remaining collisions will be elastic, wherein the molecule retains its precollision "identity" although some directional and energy changes occur. The net effect of both types of collision is to drive the particle velocity toward that of the gas; however, the inelastic collisions also cause particle heating during this equilibration.

Thus we expect the particles to be accelerated by the gas, eventually reaching the gas velocity. The time for velocity equilibration to occur will be greater, the lower the gas density (the higher the altitude). We also expect the particles to be heated by collisional energy transfer from the gas. On the other hand, the particles will be cooled by energy loss from radiation and possibly vaporization. The temperature history of the particles will be the result of the net energy exchange from these gains and losses. Eventually, when the particles are traveling at the gas speed, we expect the final particle temperature to be determined by a balance between radiative loss, and the residual collisional heating, which is just conduction.

As described previously,[1] an elegant theory is available for modeling this behavior in free molecule flow, where the fundamental parameter is the accommodation coefficient, which is the fraction of gas/particle collisions which are inelastic. Unfortunately, as either the gas density or particle size is increased, the interaction is no longer governed by this simple kinetic model. Indeed, ultimately the flow becomes continuum, where quantities such as viscosity and thermal conductivity are used to describe the aggregate effects of manifold collisions. The concept of accommodation is unimportant in this limit inasmuch as a molecule near a particle can undergo multiple collisions with the particle before leaving its environment.

For the particle sizes of interest, and altitudes between 150 and 10 km, the relevant flow regimes span the range of free molecular to continuum, and thus the free molecule theory must be extended. Regardless of the flow regime, however, the basic phenomenology described above remains the same. The basic equations which define this behavior, valid over the desired flow regimes, are outlined in the following subsection.

Particle Trajectory and Heating Equations

To describe the trajectory and heating of a particle moving through a specified flowfield, we need the equations of motion and energy for the particle.

The equation of motion is simply Newton's law relating the particle mass M_p, the particle acceleration, and the drag force on the particle D. We use a coordinate system fixed to the re-entry body, with x in the direction of the freestream flow (the wake axis) and r perpendicular to that direction. Notice that the particle moves in a plane through the axis, so we may treat x, r as a set of two-dimensional Cartesian coordinates for particle motion, even though for the flow of wake gases x and r define a cylindrical coordinate system.

The particle coordinates depend on time, and the velocity and acceleration are $\dot{x}$, $\dot{r}$ and $\ddot{x}$, $\ddot{r}$. The gas flow velocity field is defined by U_x, U_r so the velocity of the gas relative to the particles has components $U_x-\dot{x}$, $U_r-\dot{r}$. Then, the axial and radial components of the equation of motion are

$$M_p\ddot{x}=D(U_x-\dot{x})/V_{\text{rel}} \tag{1a}$$

$$M_p\ddot{r}=D(U_r-\dot{r})/V_{\text{rel}} \tag{1b}$$

where V_{rel} is the speed of the gas relative to the particles. The drag D is specified by means of a drag coefficient C_D as

$$D=0.5\,C_D\rho V^2{}_{\text{rel}}\pi R_p^2 \tag{2}$$

where ρ is the gas density and R_p the radius of the particle. The particle is taken as a sphere with density ρ_p so its mass is $M_p=4\pi R_p^3\rho_p/3$. The equations of motion (1), then become

$$\frac{d\dot{x}}{dt}=\frac{3\rho C_D V_{\text{rel}}}{8\rho_p R_p}(U_x-\dot{x}) \tag{3a}$$

$$\frac{d\dot{r}}{dt}=\frac{3\rho C_D V_{\text{rel}}}{8\rho_p R_p}(U_r-\dot{r}) \tag{3b}$$

To solve these equations we need to specify the particle properties ρ_p, R_p, the gas properties ρ, U_x, U_r, and the drag coefficient of the particle, C_D.

The energy equation for the particle makes use of the assumption that it has uniform temperature throughout its volume. Then its heat content at any particle temperature T_p is

$$\mathcal{Q}=M_p h_p,\quad h_p=\int_0^{T_p} C\,dT_p \tag{4}$$

where C is the particle specific heat per unit mass so h_p is the heat content per unit mass. The particle can gain energy from the gas by convection and conduction, which we will treat together as collisional heating (subscript "coll"). It can lose energy by radiation (subscript "rad") and also by vaporization (subscript "vap"). Thus, the change of heat content in a particle coordinate system is

$$\left(\frac{d\mathcal{Q}}{dt}\right)=\left(\frac{d\mathcal{Q}}{dt}\right)_{\text{coll}}-\left(\frac{d\mathcal{Q}}{dt}\right)_{\text{rad}}-\left(\frac{d\mathcal{Q}}{dt}\right)_{\text{vap}} \tag{5}$$

The radiation loss will be taken to correspond to a radiator with some total emissivity ϵ, so that

$$\left(\frac{d\mathcal{Q}}{dt}\right)_{\text{rad}}=4\pi R_p^2\epsilon\sigma T_p^4 \tag{6}$$

where σ is the Stefan-Boltzmann constant. Within the present model, it is assumed that for particle radius above some critical value the emissivity is a function only of T_p because the particle acts like a surface radiator. For smaller radii, the particle is taken to behave like a volume emitter with a flux proportional to R_p^3.

The vaporization energy loss is modeled by a simple evaporation mechanism. Vapor leaves the surface at a speed v_v, with density ρ_v. It carries with it energy per unit mass $h_p+\Delta H_v$, where ΔH_v is the vaporization energy per unit mass. In addition, we insert a vaporization efficiency or "sticking factor" α_v. Then we may write the vaporization loss as

$$\left(\frac{d\mathcal{Q}}{dt}\right)_{\text{vap}}=4\pi R_p^2\rho_v v_v\alpha_v(h_p+\Delta H_v) \tag{7}$$

The vapor density is obtained from the Clausius-Clapeyron equation.[3] The vaporization velocity v_v is chosen so that the mass flow of vapor, $\rho_v v_v$, is the efflux through a small hole in free-molecule flow. Thus v_v is one-quarter of the mean molecular speed at T_p.

The left term in the energy Eq. (5) is obtained by differentiating Eq. (4), and using the change in R_p found from balancing the change in mass with the vaporization mass loss,

which is

$$\frac{dR_p}{dt} = -\frac{\rho_v v_v \alpha_v}{\rho_p} \tag{8}$$

We then see that the radius change term in $d\bar{Q}/dt$ cancels the h_p term in Eq. (7).

Finally, we express the collisional heating term as a surface average rate

$$\bar{Q} = \frac{1}{4\pi R_p^2}\left(\frac{dQ}{dt}\right)_{coll} \tag{9}$$

Then we can divide the energy balance by $M_p C$ and obtain a differential equation for T_p as

$$\frac{dT_p}{dt} = \frac{3}{C\rho_p R_p}\left(\bar{Q} - \epsilon\sigma T^4{}_p - \rho_v v_v \alpha_v \Delta H_v\right) \tag{10}$$

This is the form of the energy balance we shall use. It still requires a specification of $\bar{Q}$, as well as the material properties.

In summary, there are four equations for the four variables $x(t)$, $r(t)$, $T_p(t)$ and $R_p(t)$: Eqs. (3a), (3b), (8), and (10). Besides the material properties, they contain the drag coefficient C_D, the average collisional heating $\bar{Q}$, and the flowfield quantities U_x, U_r, ρ, T (the latter will appear in C_D and $\bar{Q}$).

Drag Coefficient Correlation

The drag coefficient of spheres has been studied extensively in all flow regimes. It is a function of the Reynolds number Re and the Mach number M of the particle in the gas flow; these are based on the flow properties, the sphere diameter, and the relative velocity. The drag coefficient also depends on the temperature ratio between the particle and the flow, T_p/T.

Recently, Henderson[4] has made an extensive correlation of C_D for spheres covering the range from continuum through rarefied flow. His result is expressed as three separate formulas in the three ranges of M given by $M<1$, $M>1.75$, and $1<M<1.75$. His equations agree with the accepted forms in the limiting cases of Stokes-Oseen flow and free molecule flow, and fit the standard experimental data for the transition region between continuum and free molecule flow, and for high-speed continuum flow. Comparison with other correlations shows it to be better over the whole range of M and Re for which it is applicable and data are available.

The range of M and Re of interest here may be easily found by using the Sutherland viscosity, the U.S. Standard Atmosphere Tables,[5] and some assumed particle speeds, sizes, and temperatures. Such a calculation is made in Ref. 6 for $V_{rel} = 6\times10^5$ cm/s, $R_p = 0.5$ and 5 μm, and $T_p = 2500$ K and ambient temperature at any altitude. The results show that from 10 km up, the values of Re are below 2000, and are below unity over much of the range. At the chosen velocity, M is 20 for the ambient gas at 10 km, and 6 for the 2500 K gas. So the model of C_D (and $\bar{Q}$) must cover a range of Re from 2000 to 0, and a range of M from 20 to 0.

An examination of the applicability of Henderson's formulas to this range of M and Re is made in Ref. 6 and it is concluded that they are usable for the whole range. The actual formulas for C_D are somewhat complex and will not be given here, but can be found in Refs. 4 and 6.

Collisional Heat Transfer Correlation

The energy Eq. (10) requires an expression for $\bar{Q}$, the surface-averaged heat transfer rate for a sphere. As discussed above, the Reynolds number range of interest varies from continuum to free-molecule flow, and the Mach number range is from $M\approx25$ to 0.

The knowledge of heating of small spheres is not nearly as complete as that of drag. The reasons are not hard to see. Drag measurements can be easily made by observing the slowdown of particles fired in a ballistic range, or the forces on a sphere held in a wind tunnel. But the measurement of heating is not nearly so simple. It must be done in the wind tunnel with probes attached to the model, which makes it hard to use small models, so one must instead use very low density wind tunnels. There are a few experimental studies in the rarefied regime at subsonic[7] and supersonic[8,9] speeds up to $M=6$. These papers also include some theoretical analysis. There have also been studies of stagnation-point heating in hypersonic continuum flow (Refs. 10, 11, for example), and for the surface integral of hypersonic continuum heat transfer.[12] The free molecule heating theory is of course well-known.[13]

Based on the results of these papers, we have constructed a correlation formula that extends from continuum to free-molecule flow. It agrees with the supersonic and hypersonic continuum results at high densities, with the free-molecule results at low densities, and in the intermediate regime agrees fairly well with the available subsonic and supersonic experiments.

The detailed derivation of this correlation formula is given in Ref. 6. It is based on the use of expressions for the limiting cases of free-molecule and continuum flow, $\bar{Q}_{FM}$ and $\bar{Q}_C$. The former is obtained from Ref. 13 (after correcting an error in the denominator of Eq. (6-5) of that reference). The latter is constructed by combining the low-speed correlation of Drake[14] with the Mach number correction proposed by Fox and Nicholls.[15] The most notable feature of these limiting expressions is that $\bar{Q}_{FM}$ is proportional to the gas density ρ while $\bar{Q}_C$ scales as $\rho^{0.55}$.

The final correlation formula for $\bar{Q}$ was obtained by noticing that Kavanau [7] had proposed a formula for subsonic flow which in the limit of the velocity approaching zero could be rewritten as

$$\frac{1}{\bar{Q}} = \frac{1}{\bar{Q}_C} + \frac{1}{\bar{Q}_{FM}} \tag{11}$$

This has the correct limits for large and small ρ because of the ρ dependence mentioned above.

The validity of this formula was tested in Ref. 6 on the subsonic data of Ref. 7, up to $M=0.6$, and the supersonic data of Refs. 8 and 9 up to $M=6$. The comparison is reasonably good. For applicability to hypersonic flow another expression for $\bar{Q}_C$ was obtained, using the stagnation-point heating correlation of Ref. 10, which Perini[11] has recently found to be applicable to all available experimental data covering a simulated velocity range of 2300-17,600 m/s and a simulated altitude range of 6-52 km. To relate the stagnation-point heating to the surface-averaged heating, the results of Ref. 12 were used, with the rear hemisphere assumed to contribute nothing. The result is an expression for $\bar{Q}_C$ appropriate to high Mach number flow to use in Eq. (11).

There are no hypersonic experiments measuring $\bar{Q}_C$, so this expression cannot be evaluated there. But we can compare the use of Eq. (11) with the supersonic and hypersonic forms of $\bar{Q}_C$ and a detailed comparison is made in Ref. 6. It is shown there that the two forms agree well at hypersonic speed and since the supersonic correlation agrees with experiments it was concluded that Eq. (11), with the supersonic form of $\bar{Q}_C$ was the heating expression to use in the present work.

After the present work was completed, we found a paper by Sherman,[16] in which Eq. (11) had been proposed for use in the subsonic regime.

Wake Flowfields

With the basic tools for predicting particle heating/dynamics outlined above, it now remains to define the gaseous environment. Specifically, the flowfield quantities

U_x, U_r, T, and ρ are needed to complete the specification of the conditions in which the particle operates.

The density is determined from the perfect gas law under the condition that the pressure was well as the gases in the wake are the same as those in the freestream. Then ρ can be found from T by

$$\rho = \rho_\infty T_\infty / T \tag{12}$$

leaving only U_x, U_r and T to be specified.

We have chosen to specify these three flowfield properties by using rather simple analytical models of the axisymmetric hypersonic wakes behind sharp cones, including both laminar and turbulent wake models. They require only the specification of the general characteristics of the cone, and whether the flow is to be considered laminar or turbulent. These models are not intended to be detailed and accurate descriptions of the wake, but contain a level of sophistication appropriate to the present problem.

Wake flowfields can be quite complex, with a recirculation region close to the body, enveloped by shear layers and shockwaves. This region, of the order of the base diameter of the body, is small compared to optical lengths of interest, so we have ignored it in our wake description. We begin the wake at a point corresponding to the rear stagnation point at the back of the recirculation region, which we take as $x=0$, and continue downstream from there.

The wake flow can be either laminar or turbulent, depending upon the flow Reynolds number. This in turn depends on body length and shape, flight speed, and, primarily, on the gas density (or altitude). Although we developed models for both laminar and turbulent wakes, we did not deal with the transition from laminar to turbulent flow within the wake. The wake is taken to be either laminar or turbulent at any one flight condition. There are several reasons for this restriction. First, our interest in particle radiation is limited to a small region of the wake, say the first 30 m for example, and wake transition is only important if it occurs within that distance. Second, if one allows transition to occur, one must carefully match mass, momentum and energy fluxes, which leads to more complicated fluid mechanics than we can consider here. We do permit some generality, however, by allowing the case where the flow about the body generating the wake is laminar, while the wake is turbulent, as well as the cases of both body and wake being laminar or turbulent together.

The bodies themselves are taken as sharp cones at zero angle of attack, so the wakes are axisymmetric, and ablation effects are ignored. As mentioned above, the gas is always taken to be perfect, although the models are constructed so that the gas temperatures are appropriate to real wakes. The inclusion of the effects of nose bluntness, angle of attack, ablation, and real gases would require a degree of sophistication in the fluid mechanics which is beyond the scope of the present work.

The laminar wake model is constructed using an integral approach, a method which dates back to the early days of interest in hypersonic wakes, as for example in Ref. 17. The equations of momentum and energy in cylindrical coordinates, with the boundary layer simplifications, are integrated from $r=0$ to ∞. The dissipation term in the energy equation is neglectd because the change in U_x across the wake is small. For the same reason, the equations are linearized in U_x with some average velocity $\overline{U}$. Then a mass-weighted radius coordinate R_w is used, and the temperature and velocity profiles are assumed as Gaussian in R_w, with axial values and radial decay scales which depend on axial distance x. These four functions of x can be determined from the momentum and energy integral equations, and from the limiting forms taken by the momentum and energy differential equations on the axis. To simplify the analysis somewhat, the radial decay scales for temperature and velocity are taken to be related by the Prandtl number, which is consistent with laminar radial diffusion of energy and momentum. The initial conditions for the four functions of x are determined from the friction drag of the body, the Prandtl number relation mentioned above, and estimates for the initial axial values of T and U_x. These latter two can be considered fairly well known from the wealth of experience that exists for laminar wakes. The result of this model is a set of formulas for $T(x,r)$ and $U_x(x,r)$. The density is obtained from Eq. (12), and the radial velocity U_r is taken to be zero, since it is zero both on the axis and at radial infinity, and so is small everywhere.

For the turbulent wake, a semiempirical approach is taken, following Ref. 18, which suggests using the experimental temperature and velocity profiles of Ref. 19. They are Gaussian in the mass-weighted radial coordinate R_w, with axial velocity and temperature as unspecified functions of x, and a single radial decay length $L(x)$. The axial velocity distribution is taken from Finson,[18] who has assembled and evaluated the experimental data and recommended a curve with $x/(C_{DV}A)^{1/2}$ as independent variable, where A is vehicle base area and C_{DV} is vehicle drag coefficient. The axial temperature distribution is then found by a modified form of Reynolds' analogy. Finally, the radial decay length L is found using the relation between vehicle friction drag and wake momentum defect, as in the laminar model. The density is again found from Eq. (12) and $U_r=0$.

To complete the laminar and turbulent models we need the wake edge conditions and the vehicle total drag and friction drag coefficients. The edge conditions are found by expanding the inviscid flow on the conical body surface isentropically to the freestream pressure. The surface flow is taken from the theory of Lees[20], which agrees with Kopal[21] for small cone angles (~ 10 deg half angle) and high vehicle Mach numbers (>5). This flow is expanded to p_∞, to find the edge temperature. The edge velocity is then found by conservation of total enthalpy. However, these conditions do not apply sufficiently far from the wake centerline. There the shock system about the body has attenuated, and the flow again has the freestream properties. To simulate this in our simple wake model we choose a value of r beyond which the gas properties are taken to be freestream, regardless of the wake model. In the calculations we have made, we have chosen this distance to be five times the body base radius.

The friction drag coefficient of the body for laminar flow is taken from the correlation of Ref. 22. For turbulent flow, Finson[18] suggests that the constant value $C_{DF}=0.02$ is sufficiently accurate. The total drag coefficient is the sum of the friction drag, the pressure drag, and the base drag and Finson has also recommended a simple form for the latter two.

The wake models also require specification of several initial values. For both laminar and turbulent wakes, the initial axial temperature T_0 and the average velocity over the wake width are needed. Based on knowledge of the temperatures about slender pointed cones in hypersonic flow, we have used the value $T_0=3000$ K in our calculations. Since the velocity across the wake from axis to edge varies only slightly from U_e, the average velocity $\overline{U}$ must be close to U_e. We have performed our calculations with $\overline{U}=0.9\,U_\infty$. For the laminar wake, we also need the initial value of the axial velocity. Based again on experience with laminar hypersonic wakes about slender pointed cones, we have taken it to be 80% of the freestream speed.

A detailed derivation and description of the laminar and turbulent wake models is given in Ref. 6.

III. Results and Discussion

The model that has been described was incorporated into a computer program and used to calculate the trajectories, temperature history, and radiation from small particles composed of carbon, silicon carbide, and tungsten carbide. The thermodynamic and radiative properties of these

materials were taken from the best available data, as described in Ref. 6.

Calculations were performed for particles of radius between 1 and 10 μm, injected from the center of the base of the re-entry vehicle at a velocity of 3×10^4 cm/s relative to the vehicle. The particles, when injected, were taken to be either cold (300 K) or heated (2500 K), and the angle of injection, measured from the wake axis varied from 0 to 60 deg. The gaseous flowfields into which the particles were injected were described by the analytical model of either a laminar or turbulent wake described above. Wakes down to 45 km were taken as laminar; below 45 km they were taken as turbulent. The body was taken to be a slender pointed cone (9 deg half angle) of typical size, on a trajectory with re-entry angle 20 deg and re-entry velocity 6.6. km/s.

All effects due to the plume of gases by which the particles are injected have been neglected, as have the near wake regions such as the recirculation region. Justifications for the validity of these assumptions are presented in Ref. 6.

Typical particle temperature predictions at various altitudes are shown vs distance downstream in Fig. 1. The case shown corresponds to cold 1 μm radius carbon particles injected along the wake axis. The altitude dependence of the temperature histories is quite instructive. Above approximately 90 km, the predicted increases in particle temperature are minimal, indicating that the particle/gas regime is near or in the exoatmospheric limit (no interaction). Below 90 km the particle temperatures exhibit a maximum within the first 100 m of wake. This maximum occurs even though the relative velocity between particle and gas is still large over the range of distance shown. The reason for this is that collisional heating is proportional to gas density, whereas particle radiative loss scales strongly with temperature. Thus, even if the relative velocity remains large, at high altitudes a particle temperature will be reached where collisional heating can at best only balance radiative loss, and at this point a temperature maximum will occur. With increasing distance beyond this point, the relative velocity slowly decreases through collisions, and thus particle temperature decreases also.

With decreasing altitude the rate of collisional heating increases and the maximum temperature becomes higher and occurs closer to the vehicle (the relative velocity decreases more rapidly also). At altitudes of 40-60 km a different phenomenon starts to become dominant; as particle deceleration becomes more rapid, a situation arises where the relative velocity becomes so low that the recovery temperature falls below the particle temperature. When this occurs gas/particle collisions will lead to convective cooling rather than heating. This effect clearly dominates near the body at the lowest altitudes shown. Indeed, below 30 km, conductive effects dominate at distances beyond that of peak particle temperature, and thus the particle temperatures are found to track those of the wake.

Particle radiation calculations for the case of Fig. 1 are shown in Fig. 2. The predictions are for the total radiation per unit particle mass flow in the first 30 m of wake, and are shown for four bandpasses which span the near to long wavelength infrared. The distance of 30 m was taken as representative of the characteristic spatial resolution of an optical monitoring system. For these 1 μm carbon particles the spectral emissivities of the four bandpasses were taken from Ref. 23, where they were calculated using Mie theory. The values are 1.0, 1.6, 0.9, and 0.35 in order of increasing wavelength. It should be noted that the total radiation is a function not only of the particle temperature history, but also of the time the particle remains within the field-of-view. This residence time decreases with decreasing altitude because of the changing particle velocity history. The predicted radiation shown at 150 km may be regarded as the exo-atmospheric limit and any change from these values is a result of the gas/particle interaction. It can be seen that peak radiation enhancements of order 3-10 occur for the longest wavelength bands in the altitude range 40-90 km. The radiation in these bands begins to drop at the lowest altitudes; indeed, the radiation for the 18.0-21.9 μm band is essentially the same at 10 and 150 km. In essence then, at the longest wavelength considered, the difference in particle temperatures between 10 and 150 km is almost completely compensated for by the

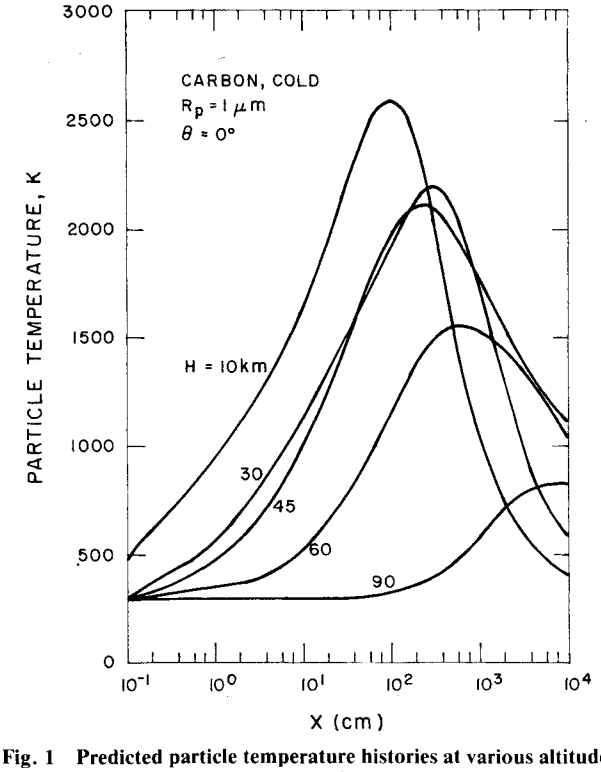

Fig. 1 Predicted particle temperature histories at various altitudes as a function of downstream distance. Carbon, $R_p = 1$ μm, $T_{p_0} = 300$ K, wake centerline injection.

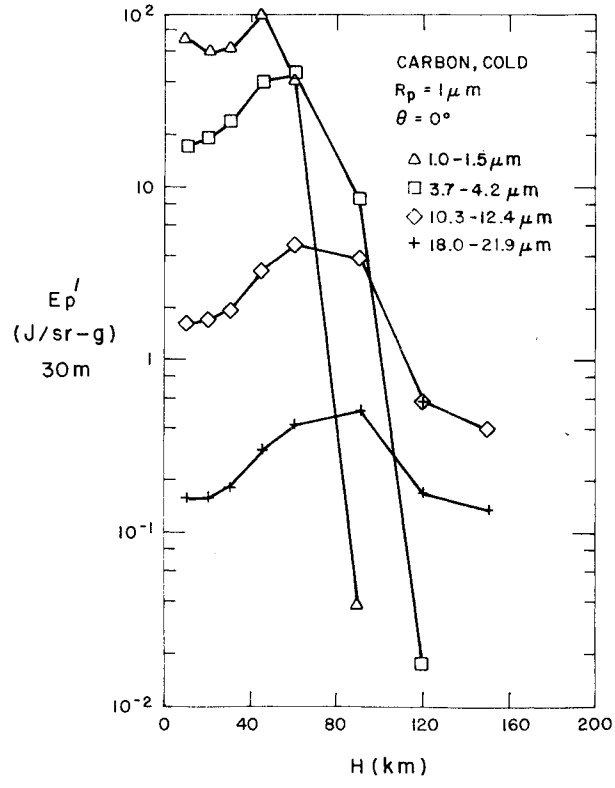

Fig. 2 Predicted radiation per unit mass flow in first 30 m of wake. Bandpasses as shown; conditions as in Fig. 1.

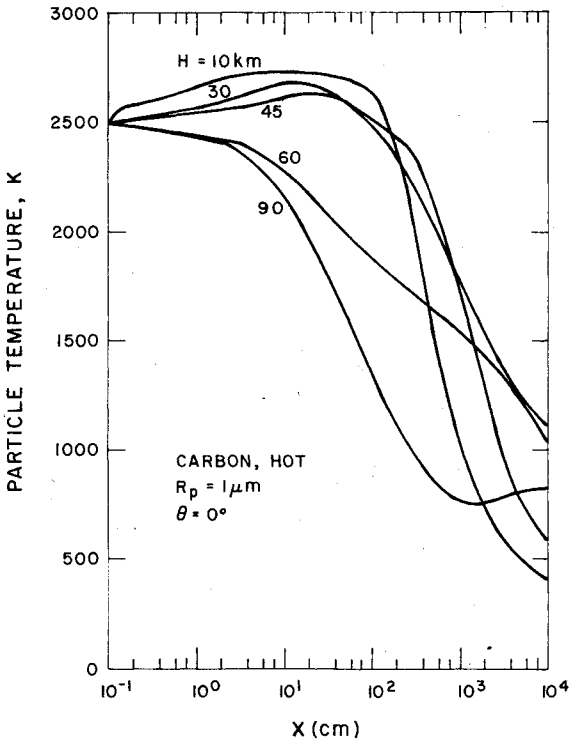

Fig. 3 Predicted particle temperature histories at various altitudes as a function of downstream distance. Carbon, $R_p = 1$ μm, $T_{p_0} = 2500$ K, wake centerline injection.

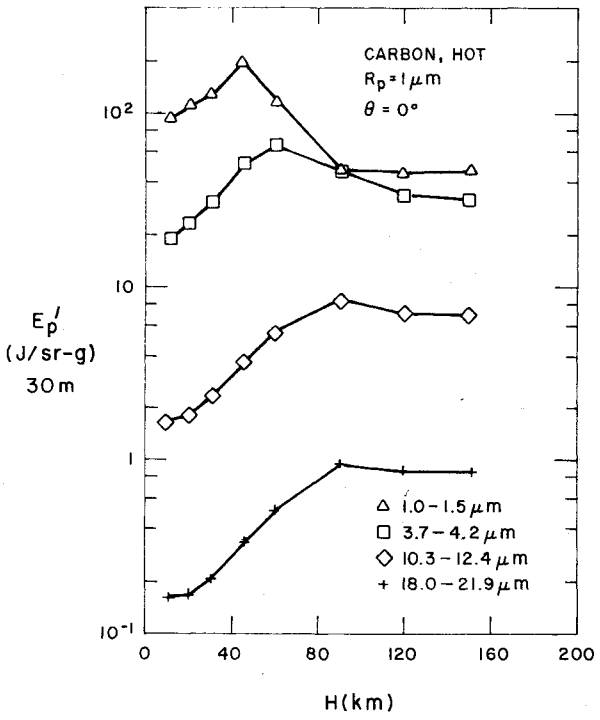

Fig. 4 Predicted radiation per unit mass flow in first 30 m of wake. Bandpasses as shown; conditions as in Fig. 3.

change in residence time; i.e., the particle recedes from the vehicle at near U_∞ at 10 km, and at the much slower injection velocity at 150 km. In the lower wavelength bands the radiation enhancement is many orders of magnitude, reflecting the exponential dependence of the Planck function with temperature at these wavelengths. The peak radiation level in these bands occurs at altitudes near wake transition; however, even at 10 km, the short wavelength infrared band radiation is at most only a factor of two below the peak value.

Predicted temperature histories for the case of heated 1 μm radius carbon particles injected along the wake axis are presented in Fig. 3. At the highest altitudes shown, the particle temperature decreases solely because of radiative losses; particle heating first becomes evident at an altitude of 90 km. At the lower altitudes slight increases in particle temperature are observed close to the body. The far wake temperature histories at these altitudes are found to be similar to those for cold carbon particles (Fig. 1). Radiation predictions for this case are shown in Fig. 4 and are found to be very similar to those of cold carbon particles (Fig. 2) at altitudes below ≈60 km. On the other hand, the predicted high altitude radiation signatures for heated particles are much larger than those for cold particles, reflecting their higher initial heat content. Note that in the case of heated particles there is no significant radiation enhancement in the LWIR. Indeed, in this case, the predictions for an altitude of 10 km are a factor of five below those for 150 km. Again this behavior reflects the reduced particle residence time within the field-of-view at the lower altitude. Similar behavior is observed for 5 and 10 μm heated particles.

The predictions shown in Figs. 1-4 are typical of those realized for other particle sizes, materials and injection modes. However, a number of important phenomenological features of the particle/gas interaction have become apparent from an examination of many such calculations.[6] Specifically, it has been found that: 1) for grey body radiators, an increase in particle size generally results in a decrease in radiation efficiency (defined as radiation per unit mass flow); 2) peak particle temperatures are found to increase with particle density; however, in terms of radiation efficiency, this increased particle temperature is insufficient to compensate for the increased particle mass; this trend can reverse at low wavelengths, $\lesssim 1\mu$m, because of the exponential dependence of the Planck function with temperature in this wavelength region; 3) injecting heated particles is only advantageous at altitudes $\gtrsim$ 60 km; 4) injecting into the free-stream or inviscid wake is only advantageous at altitudes $\gtrsim$ 60-80 km and indeed is difficult to do at lower altitudes; 5) at low altitudes there is no significant radiation enhancement in the LWIR and in fact, for the case of injection of heated particles, the low altitude LWIR signatures can be notably smaller than the exo-atmospheric values.

IV. Summary

In summary, a model has been developed for predicting the radiation signatures of small particles injected into re-entry flowfields. The model incorporates the interaction between the particle and ambient gas streams and is applicable over the full range of free molecular to continuum flows and hypersonic to thermal velocities. The model includes convective/conductive heat transfer between particle and gas, as well as particle radiative and evaporative losses, and predicts both particle trajectories and temperature histories. The flowfield into which the particle is injected has been modeled as the laminar or turbulent wake of a pointed cone in axisymmetric flow, by using simple analytical expressions for density, temperature and velocity. They are obtained by the use of integral solutions of the wake flow equations, which are related to the drag of the body and initial conditions for hypersonic wakes.

The model has been exercised for several materials over a range of particle sizes and injection conditions. The changes in particle signature which occur when particle injection angle, size or initial temperature are varied have been delineated and optimum injection conditions have been defined as a function of altitude.

It has been found that the highest altitude at which particle/flow field interactions can affect particulate radiation signatures will be between 90-120 km depending upon a number of variables such as particle properties, injection

configuration, re-entry vehicle size and radiation wavelength. Furthermore, at altitudes above approximately 60 km, the choice of particle injection mode (i.e., angular or axial, heated or cold) can provide for significant variations in radiation efficiency, with the optimum configuration being the injection of heated particles at an angle relative to the flow axis. Below altitudes of approximately 60 km, the particle behavior is controlled more by the gas-particle interactions rather than the initial injection conditions. Indeed, it has been found that there is no longer an advantage in injecting heated particles at altitudes below 60 km. Lastly, it was seen that at altitudes below approximately 30 km, small particles will essentially equilibrate with the flow within a few meters downstream of the body.

In terms of radiation efficiency, it has been shown that particle-gas interactions can provide for significant increases in radiation levels over those achieved under exo-atmospheric conditions. This is particularly true for the lower wavelengths considered. On the other hand, no radiation enhancements have been predicted for the long wavelength infrared. Indeed, for the case of injection of heated particles, it has been observed that predicted radiation levels at low altitudes are significantly smaller than those predicted for exo-atmospheric conditions. The total particle radiant intensity is controlled by the particle temperature history and the particle residence time within the field of view. At low altitudes, the particle residence time is shortened because of the rapid velocity equilibration between particle and gas. This rapid equilibration can also provide elevated particle temepratures; however, in the LWIR, the temperature increase is insufficient to counterbalance the effect of shortened residence time because of the exponential temperature dependence of the Planck function.

Acknowledgment

This research was supported by the USAF Space and Missile Systems Organization under contract F04701-77-C-0088 and monitored by R. Burgess; M. Finson provided significant contributions to the development of the wake models.

References

[1] Caledonia, G. E., "Infrared Signature Modifications," Physical Sciences Inc., Woburn, Mass., TR-48, March 1976.

[2] Hall, D. R., "Hypersonic Free-Molecular Heating of Micron Size Particulate," *AIAA Journal*, Vol. 16, Aug. 1978, pp. 857-859.

[3] Glasstone, S., *Thermodynamics for Chemists*, D. Van Nostrand Co., New York, N.Y., 1950, p. 227.

[4] Henderson, C. B., "Drag Coefficients of Spheres in Continuum and Rarefied Flows," *AIAA Journal*, Vol. 14, June 1976, pp. 707-708, and "Reply by Author to M. J. Walsh," *AIAA Journal*, Vol. 15, June 1977, pp. 894-895.

[5] *U.S. Standard Atmosphere, 1976*, Government Printing Office, Washington, D. C., 1976.

[6] Caledonia, G. E., Kemp, N. H., and Simons, G. A., "Endo Optical Masking Studies, Final Technical Report," Physical Sciences Inc., Woburn, Mass., TR-125 (SAMSO TR-78-95), July 1978.

[7] Kavanau, L. L., "Heat Transfer from Spheres to a Rarefied Gas in Subsonic Flow," *Transactions of ASME*, Vol. 77, July 1955, pp. 617-623.

[8] Drake, R. M., Jr., and Backer, G. H., "Heat Transfer from Spheres to a Rarefied Gas in Supersonic Flow," *Transactions of ASME*, Vol. 74, Oct. 1952, pp. 1241-1249.

[9] Eberley, D. K., "Forced Convection Heat Transfer from Spheres to a Rarefied Gas," U. Cal. Inst. Eng. Research, Berkeley, Calif., Rept. HE-150-140, July 1956.

[10] Detra, R. W., Kemp, N. H., and Riddell, F. R., "Addendum to 'Heat Transfer to Satellite Vehicles Re-entering the Atmosphere', " *Jet Propulsion*, Vol. 27, Dec. 1957, p. 1256.

[11] Perini, L. L., "Compilation and Correlation of Stagnation Convective Heating Rates on Spherical Bodies," *AIAA Journal*, Vol. 12, March 1975, pp. 189-191.

[12] Kemp, N. H., "Note on the Surface Integral of Laminar Heat Flux to Symmetric Bodies at Zero Incidence," *ARS Journal*, Vol. 32, April 1962, pp. 639-640.

[13] Schaaf, S. A., and Chambre, P. L., "Flow of Rarefied Gases," *Fundamentals of Gas Dynamics*, H. W. Emmon, Ed., Princeton University Press, Princeton, N. J., 1958, Sec. H.

[14] Drake, R. M. Jr., "Discussion," *Journal of Heat Transfer*, Vol. 83, May 1961, pp. 170-172.

[15] Fox, T. W., and Nicholls, J. A., "Ignition of Magnesium Powders in Shock Wave Induced Flows," Combustion Institute, Cleveland, Ohio, 1977.

[16] Sherman, F. S., "A Survey of Experimental Results and Methods for the Transition Regime of Rarefied Gas Dynamics," *Rarefied Gas Dynamics, Third Symposium,* Vol. II, Academic Press, New York, 1965, pp. 228-260.

[17] Feldman, S., "On the Trails of Axisymmetric Hypersonic Blunt Bodies Flying Through the Atmosphere," *Journal of the Aerospace Sciences*, Vol. 28, June 1961, pp. 443-448, 470.

[18] Finson, M. L. "Density Distribution in Supersonic Projectile Wakes," Physical Sciences Inc., Woburn, Mass., TR-66, Oct. 1976.

[19] Demetriades, A., "Mean-Flow Measurements in an Axisymmetric Compressible Turbulent Wake," *AIAA Journal*, Vol. 6, March 1968, pp. 432-439.

[20] Lees, L., "Note on the Hypersonic Similarity Law for an Unyawed Cone," *Journal of the Aeronautical Sciences*, Vol. 18, Oct. 1951, pp. 700-702.

[21] Kopal, Z., *Tables of Supersonic Flow Around Cones,* MIT, Dept. of Electrical Engineering, Cambridge, Mass., 1947, p. 472.

[22] Kohrs, R., Pannabecker, C., Patay, S., and Wells, D., "The Determination of Hypersonic Drag Coefficients for Cones, Biconics, and Triconics," Avco Missile Systems Division, Wilmington, Mass., AVMSD-0136-67-CR, March 1967.

[23] Dowling, J. M., and Randall, C. M., "Infrared Emissivities of Micron-Sized Particles of C, MgO, Al_2O_3 and ZrO_2 at Elevated Temperatures," Air Force Rocket Propulsion Laboratory, Edwards Air Force Base, Calif., AFRPL-TR-77-14, April 1977.